[Supplementary Information]

Fe incorporated α-Co(OH)$_2$ with remarkably improved activity and stability towards oxygen evolution

Haiyan Jin, Shanjun Mao, Guopeng Zhan, Fan Xu, Xiaobing Bao and Yong Wang*

Advanced Materials and Catalysis Group, ZJU-NHU United R&D Center, Center for Chemistry of High-Performance and Novel Materials, Key Lab of Applied Chemistry of Zhejiang Province, Department of Chemistry, Zhejiang University, Hangzhou 310028, P. R. China.

Experimental Details

Materials. cobalt(II) nitrate hexahydrate ($Co(NO_3)_2$•$6H_2O$), Iron(III) nitrate nonahydrate ($Fe(NO_3)_3$•$9H_2O$), Sodium nitrate ($NaNO_3$), Ammonium fluoride (NH_4F), Sodium Citrate, 5 wt.% Nafion 117 solution and Commercial IrO_2 were purchased from Aladdin. 2-propanol and potassium hydroxide (KOH) were from Sinopharm Chemical Reagent Co., Ltd. High-purity water (18.25 MΩ·cm) supplied by a UP Water Purification System was used in all the experiments.

Preparation of β-Co(OH)$_2$: $Co(NO_3)_2$•$6H_2O$ (0.5 M, 1.12mL) were dispersed in 100 mL H_2O (purged with N_2). The NaOH solution (0.08 M, 40mL, purged with N_2 for 30 min) was dropped into the above solution at a rate of 5 μL s^{-1}. Then, the resulting solution was continuously heated until it became to be pink. The as-obtained solution was continued to be stirred for more than 12h. The solid product was collected by centrifugation and washed. The preparation of Fe-incorporated β-Co(OH)$_2$ is similar to that of β-Co(OH)$_2$ except that $Co(NO_3)_2$•$6H_2O$ and $Fe(NO_3)_3$•$9H_2O$ as metal precursors. As shown in the XRD pattern from Fig. S1 (SI), β-$Co_4Fe(OH)_x$ consists of β-Co(OH)$_2$ and CoFe-LDH (for convenience, we call it β-$Co_4Fe(OH)_x$), that is, some Fe cannot be incorporated into β-Co(OH)$_2$.

Synthesis of spinel Co_4FeO_x: α-$Co_4Fe(OH)_x$ was calcinated at 400 °C for 3h in air. The as-obtained black powder was spinel Co_4FeO_x.

Electrochemical characterizations: The electrochemical tests were carried out in a conventional three-electrode electrochemical cell by using a CHI750E. The electrochemical impedance spectroscopy (EIS) measurements were carried out by applying Gamry reference 600 instrument. A commercial glassy carbon electrode (GCE, 5 mm diameter, 0.196 cm^2) was served as the working electrode. The presented current density referred to the geometric surface area of the glassy carbon electrode. Most OER datas have been Ohmic drop corrected based on impedance spectroscopy. The LSV curves in Fig. 2a and b have been corrected based on impedance spectroscopy. Compared to the original data, the variation of the iR-corrected

data for α-$Co_4Fe(OH)_x$) and α-$Co(OH)_2$ towards OER is evident as seen from Fig. S2 (SI). The influence of different loadings for α-$Co_4Fe(OH)_x$ on OER activity was also investigated. As expected, higher loadings result in a better performance for oxygen production (Fig. S3, SI). However, the catalysts can't perform even better when the metal loading weight overtakes 0.28 mg cm^{-2} due to partial covered active sites (Figure S3, SI). A saturated calomel electrode (SCE) and carbon rod were used as the reference electrode and the counter electrode, respectively. The catalysts was cycled about 10 times of cyclic voltammetry (CV) until a stable CV curve was developed before measuring linear sweep voltammetry (LSV) at a scan rate of 20 mV s^{-1}. The reference samples include α-$Co(OH)_2$, β-$Co(OH)_2$, β-$Co_4Fe(OH)_x$ (Fe doped β-$Co(OH)_2$), spinel Co_4FeO_x (synthesized by calcinating α-$Co_4Fe(OH)_x$) at 400 °C for 3 h), FeOOH and commercial IrO_2 nanoparticles.

Table S1. Co/Fe atomic ratio determined by ICP-AES.

Samples	Different ratio of Fe incorporated α-Co(OH)$_2$						Fe incorporated β-Co(OH)$_2$
atomic ratio of Co: Fe in the starting materials	5:1	4:1	3:1	2:1	1:1	1:3	4:1
atomic ratio of Co: Fe in the as-prepared catalyst	5.06:1	3.97:1	3.05:1	2.01:1	1.04:1	1:2.98	4.29:1

Table S2. the calculated TOF value of α-$Co_4Fe(OH)_x$, α-$Co(OH)_2$ and IrO_2.

Samples	α-$Co_4Fe(OH)_x$	α-Co(OH)$_2$	IrO_2
TOF	$27*10^{-3}$	$2.29*10^{-3}$	$5.1*10^{-3}$

Table S3. Comparison of OER activity of the α-$Co_4Fe(OH)_x$ nanosheets with recently reported catalysts.

Electrocatalyst	Electrolyte	Overpotential at 10 mA·cm^{-2} (mV)	Mass loading (mg·cm^{-2})	Reference
$NiCo_{2.7}(OH)_x$	1 M KOH	350	0.2	Adv. Energy Mater. **2015**, 1401880
FeNi-GO hybrids	1 M KOH	210	0.25	Angew. Chem. 2014, 126, 7714 –7718
CoCo-LDH-ultrathin nanosheets	1 M KOH	350	0.07	Nat. Commun. 2014, 5, 4477-4485
CoNi-LDH-ultrathin nanosheets	1 M KOH	334	0.07	Nat. Commun. 2014, 5, 4477-4485
NiFe-LDH-ultrathin nanosheets	1 M KOH	304	0.07	Nat. Commun. 2014, 5, 4477-4485
CoMn-LDH	1 M KOH	324	0.14	J. Am. Chem. Soc. 2014, 136, 16481−16484
FeNC sheets/NiO	0.1M KOH	390	0.24	Angew. Chem. Int. Ed. 2015, 54, 10530 –10534
γ-CoOOH nanosheet	1 M KOH	300	0.15	Angew. Chem. Int. Ed. 2015, 54, 8722 –8727
α-$Ni(OH)_2$ hollow spheres	0.1 M KOH	331	0.2	J. Am. Chem. Soc. 2014, 136, 7077−7084
α-$Co_4Fe(OH)x$	1 M KOH	295	0.28	this work
Fe–mCo_3O_4	1 M KOH	380	0.07	Chem. Commun. 2014, 50, 10122-10125

Table S4. Variation of Co/Fe atomic ratio of α-$Co_4Fe(OH)_x$ during OER catalysis.

OER time	0h	10h
ICP atomic ratio (Co:Fe)	3.97:1	4.18:1

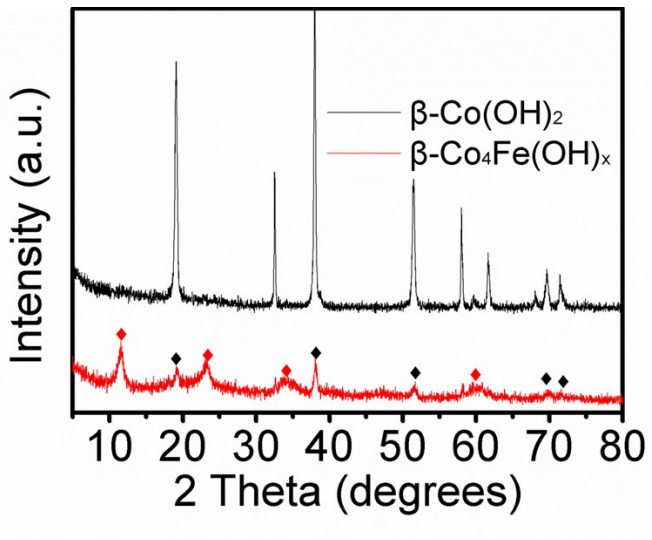

Fig. S1. the X-ray diffraction (XRD) patterns of β-$Co(OH)_2$ and β-$Co_4Fe(OH)_x$ (♦-β-$Co(OH)_2$, ♦ -LDH phase).

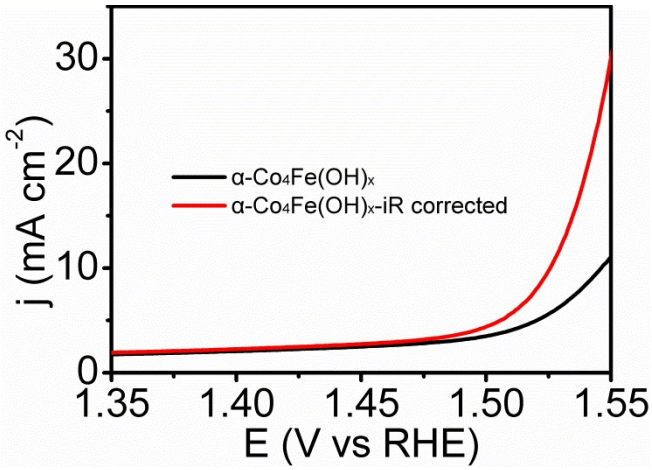

Fig. S2. The comparison of the original data and iR-corrected data for α-$Co_4Fe(OH)_x$ towards OER.

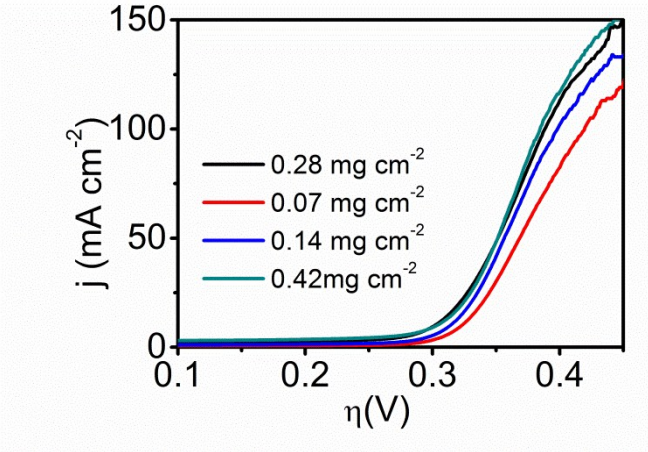

Fig. S3. Polarization curves of α-$Co_4Fe(OH)_x$ at different loading weight, suggesting the optimized loading weight for OER is 0.28 mg cm^{-2}.

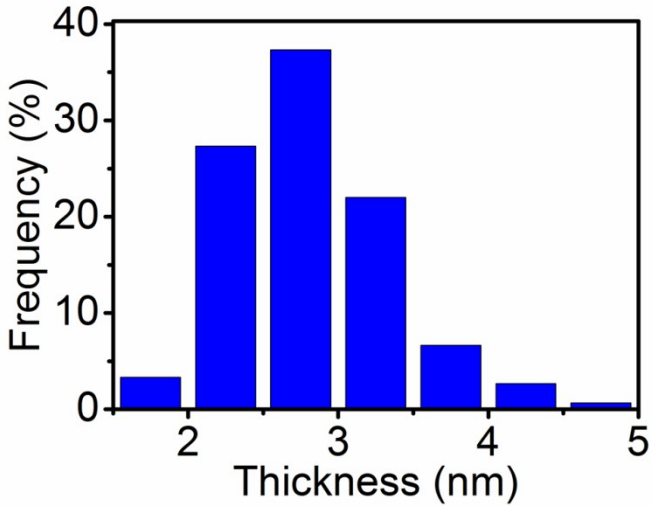

Fig. S4. Thickness distribution obtained by measuring 150 upstanding nanoplates using HRTEM.

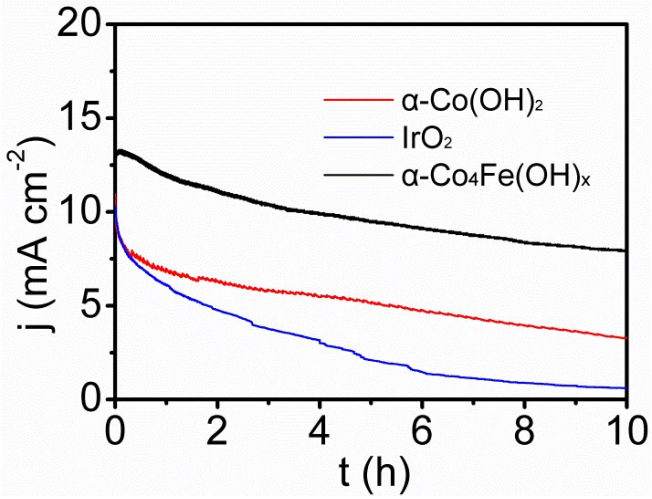

Fig. S5. Chronoamperometric curves of different catalysts for OER.

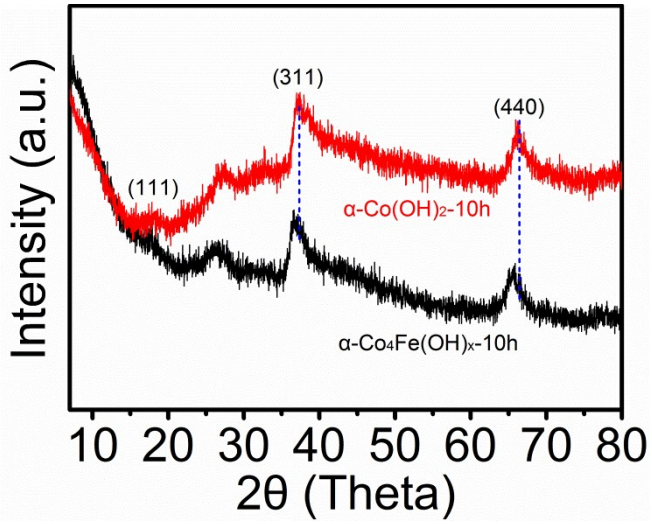

Fig. S6. The XRD pattern of α-$Co_4Fe(OH)_x$ and α-$Co(OH)_2$ after 10h OER.

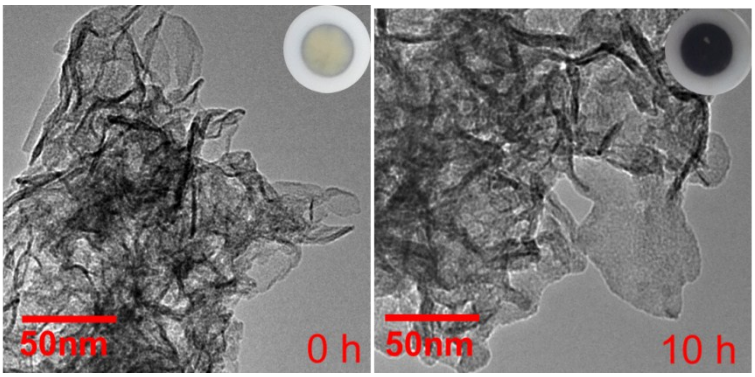

Fig. S7. the tem images (the color variation in the inset) comparison of α-$Co_4Fe(OH)_x$ prior to and after OER.

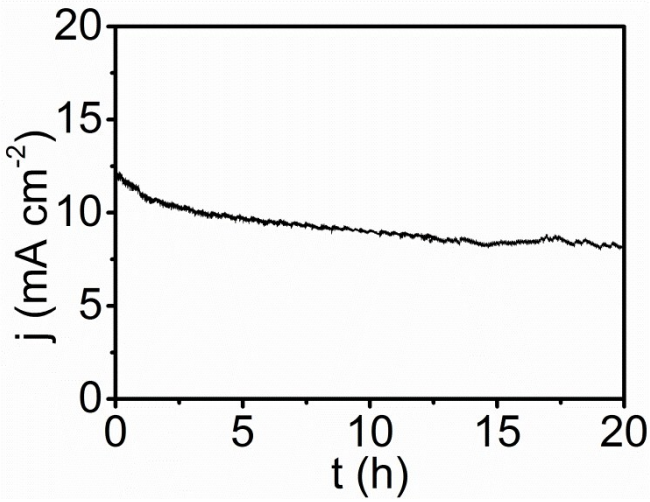

Fig. S8. Chronoamperometric curves of α-$Co_4Fe(OH)_x$ for OER 20h.

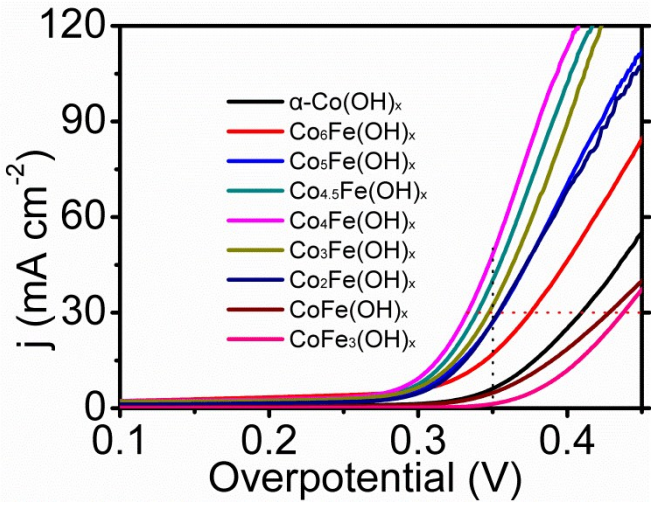

Fig. S9. LSV curves for OER of different Co/Fe ratio catalysts.

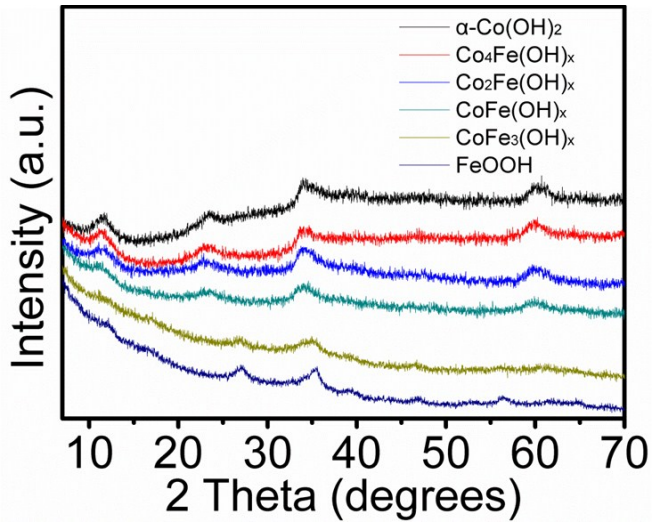

Fig. S10. the X-ray diffraction (XRD) patterns of different Co/Fe ratio catalysts.

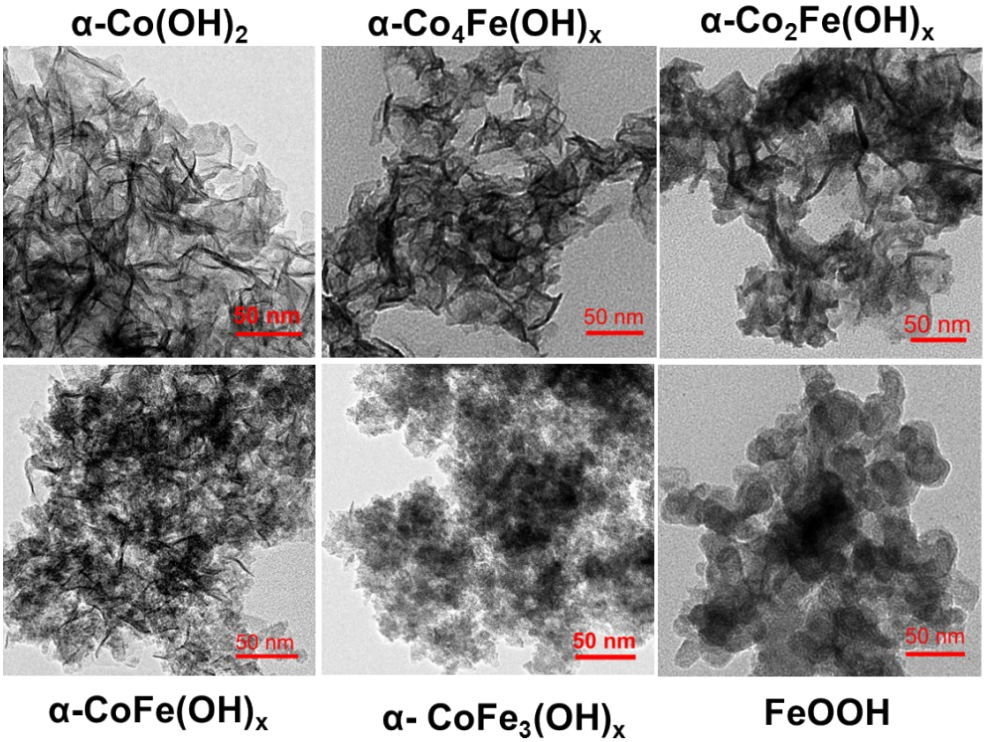

Fig. S11. The TEM images of different Co/Fe ratio.

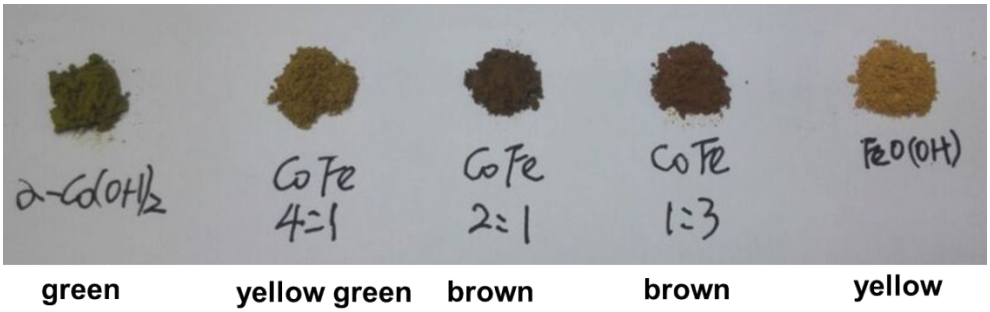

Fig. S12. the colors comparison of different Co/Fe ratio.

Capacitance measurements and relative comparison of active surface area

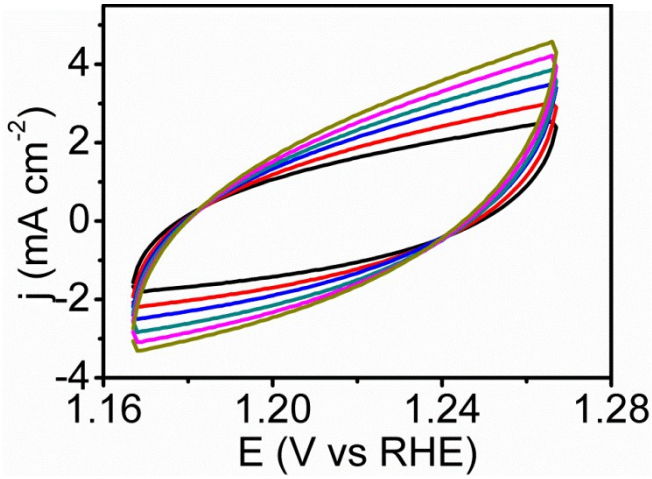

Fig. S13. Typical cyclic voltammetry curves of α-$Co(OH)_2$ in 1 M KOH with different scan rates

The estimation of the effective active surface area of catalysts was realized according to literature. Cyclic voltammetry (CV) were carried out at various scan rates (60, 80, 100 mV s^{-1}, etc.) in 1.167-1.267 V vs RHE region. The double-layer capacitance (C_{dl}) of two samples can be determined from the cyclic voltammograms, which is expected to be linearly proportional to the effective surface area (Figure 4b). The

exact determination of the surface area is difficult due to the unknown capacitive behavior of catalysts, but we can safely estimate the relative surface areas. CV measurements performed in the region of 1.167-1.267 V vs RHE could be mostly considered as the double-layer capacitive behavior. The double-layer capacitance is estimated by plotting the $\Delta J=J_a-J_c$ at 1.217 V vs RHE against the scan rate, where the slope is twice C_{dl} (Figure 4b). The calculated values of double-layer capacitance are 18.63 and 17.05 mF cm^{-2} for α-$Co_4Fe(OH)_x$ and α-$Co(OH)_2$, respectively. Since the C_{dl} is proportional to the surface area and the conductivity of the materials, more effective active sites can be exposed for α-$Co_4Fe(OH)_x$, which is responsible for the excellent OER activity.

Computational section

Calculations were performed by using periodic, spin-polarized DFT as implemented in Vienna ab initio program package (VASP).[1, 2] The electron-ion interactions were described by the projector augmented wave (PAW) method proposed by Blöchl[3] and implemented by Kresse[4]. RPBE functional[5] was used as exchange-correlation functional approximation and a plane wave basis set with an energy cutoff of 400 eV was chosen. Hubbard-U correction (DFT+U method) was applied to improve the description of localized Co d-electrons in the LDH[6]. A value of U = 3.52 eV was set since this value is considered reasonable[7, 8]. A Single layer slab (containing 88 atoms) with (33-5) surface cleavaged as the active surface was modeled (see Figure S12). A Monkhorst−Pack k-point mesh of 1*2*1 is used for the Brillouin zone sampling during the structure optimization. The periodic condition is employed along the y direction. The vacuum space along the z direction was set to be 15 Å. For Fe doped α-$Co(OH)_2$, one surface Co atom was substituted by Fe. All atoms in the supercell are allowed to relax during the structure optimization. The relaxation is stopped when the force residue on the atom is smaller than 0.02 eV/Å.

The binding energies of the intermediates O*, HO*, were calculated with the following equations:

$$\Delta E_{O*} = E(O*) - E(*) - (E_{H_2O} - E_{H_2}),$$

$$\Delta E_{HO*} = E(HO*) - E(*) - (E_{H_2O} - 1/2E_{H_2}),$$

where $E(*)$, $E(O*)$ and $E(HO*)$ are the energies of the clean surface and the surfaces with O*and HO* adsorbed, respectively. E_{H_2O} and E_{H_2} are the calculated energies of H_2O and H_2 molecules in the gas phase.

The standard gibbs free energy the intermediates O*, HO*, were defined as follows:

$\Delta G^0_{int*} = \Delta E_{int*} + \Delta ZPE - T\Delta S$,

Where ΔE_{int*}, ΔZPE and ΔS are the binding energy, zero point energy change and entropy change of the intermediate adsorbed, respectively. The values of ΔZPE and ΔS of the related intermediates are obtained in the former work of Norskov.[9]

The theoretical overpotential (η^{the}) at standard conditions is given by the equation below: [10]

$\eta^{OER} = \{\max[(\Delta G^0_{O*} - \Delta G^0_{HO*}), 3.2\ eV] - (\Delta G^0_{O*} - \Delta G^0_{HO*})/e\} - 1.23\ V$, so η^{the} *of* α-$Co(OH)_2$ is -0.67V and that of Fe doped α-$Co(OH)_2$ is -0.62V.

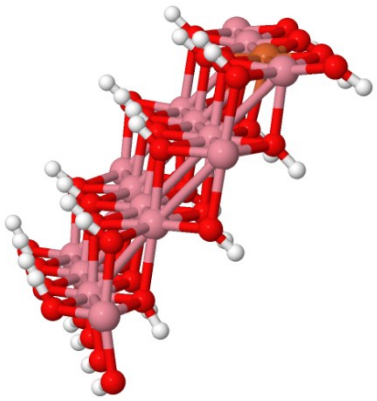

Fig. S14. unoptimized model used for OER calculation. Red: oxygen; pink: Cobalt; brown: Ferrum; white: hydrogen.

References

1. G. Kresse and J. Furthmüller, *Comp. Mater. Sci.*, 1996, **6**, 15-50.
2. G. Kresse and J. Furthmüller, *Phys. Rev. B*, 1996, **54**, 11169-11186.
3. P. E. Blöchl, *Phys. Rev. B*, 1994, **50**, 17953-17979.
4. G. Kresse and D. Joubert, *Phys. Rev. B*, 1999, **59**, 1758-1775.
5. B. Hammer, L. B. Hansen and J. K. Nørskov, *Phys. Rev. B*, 1999, **59**, 7413-7421.
6. A. I. Liechtenstein, V. I. Anisimov and J. Zaanen, *Phys. Rev. B*, 1995, **52**, R5467-R5470.
7. M. García-Mota, M. Bajdich, V. Viswanathan, A. Vojvodic, A. T. Bell and J. K. Nørskov, *J. Phys. Chem. C*, 2012, **116**, 21077-21082.
8. D. Friebel, M. W. Louie, M. Bajdich, K. E. Sanwald, Y. Cai, A. M. Wise, M. J. Cheng, D. Sokaras, T. C. Weng, R. Alonso-Mori, R. C. Davis, J. R. Bargar, J. K. Norskov, A. Nilsson and A. T. Bell, *J. Am. Chem. Soc.*, 2015, **137**, 1305-1313.
9. J. K. Nørskov, J. Rossmeisl, A. Logadottir, L. Lindqvist, J. R. Kitchin, T. Bligaard and H. Jónsson, *J. Phys. Chem. B*, 2004, **108**, 17886-17892.
10. I. C. Man, H.-Y. Su, F. Calle-Vallejo, H. A. Hansen, J. I. Martínez, N. G. Inoglu, J. Kitchin, T. F. Jaramillo, J. K. Nørskov and J. Rossmeisl, *ChemCatChem*, 2011, **3**, 1159-1165.